Mechanistic Aspects and Reaction Pathways for Oxidative Coupling of Methane on $Mn/Na_2WO_4/SiO_2$ Catalysts

Kazuhiro Takanabe[†] and Enrique Iglesia*

Department of Chemical Engineering, University of California at Berkeley, Berkeley, California 94720

Received: January 6, 2009; Revised Manuscript Received: March 15, 2009

Kinetic and isotopic methods were used to determine the identity, rate constants, and reversibility of elementary steps for primary and secondary reactions involved in the oxidative coupling of methane (OCM) on $Mn/Na_2WO_4/SiO_2$. We provide evidence in this study for parallel C−H bond activation pathways, in which H-abstraction is mediated by either oxygen species on surfaces or by OH radicals formed via H_2O/O_2 equilibration on catalyst surfaces. OCM rates and C_{2+} yields are higher when H_2O is present and OH-mediated pathways prevail, because of the high reactivity of OH radicals and of their lesser sensitivity to the energy of the C−H bond containing the hydrogen abstracted. These coupled homogeneous-catalytic sequences account for all observed kinetic effects of O_2, CH_4, and H_2O on rates and selectivities for both CH_4 conversion and for subsequent reactions of C_2H_6, C_2H_4 and C_3 products; they are also consistent with measured kinetic and thermodynamic isotope effects for C−H bond activation mediated by surface and OH radicals. Kinetic isotope effects and isotopic scrambling studies (CD_4/CH_4; D_2O/H_2O; $^{18}O_2/^{16}O_2$) indicate that C−H bond activation is irreversible and kinetically-relevant. O_2 dissociation is quasi-equilibrated, but becomes irreversible as H_2O/O_2 ratios increase with increasing conversion and residence time. Competitive reactions of $^{13}CH_4/O_2$ with $^{12}C_2H_6$, $^{12}C_2H_4$, and $^{12}C_3H_6$ with and without added H_2O show that H-abstraction from hydrocarbons is much less sensitive to C−H bond strength when OH radicals are used to abstract hydrogen instead of oxide surfaces. Maximum C_{2+} yields require conditions that favor OH-mediated pathways while maintaining equilibrium oxygen surface coverages and OH radical concentrations. OH-mediated pathways are more sensitive to O_2 pressure than surface-mediated pathways; thus, low O_2 pressures and staging strategies that maintain stoichiometric O_2 requirements and low local O_2 pressures can improve C_{2+} selectivities but only when OH radicals are maintained at equilibrium concentrations via catalytic H_2O-O_2 reactions. These findings and interpretations indicate that intermediate O_2 pressures give maximum C_{2+} yields, but that their optimal value depends sensitively on prevalent H_2O concentrations as they vary with conversion along the reactor. These predictions about the consequences of various operating strategies have become feasible because of the detailed and quantitative nature of the mechanism-based kinetic networks reported here for the first time.

1. Introduction

The oxidative coupling of methane (OCM) involves the conversion of CH_4–O_2 mixtures to higher hydrocarbons[1,2] and benefits from the avoidance of sequential steps required in indirect routes involving CH_4 reforming and Fischer–Tropsch synthesis,[3] while producing light alkenes, which cannot be formed via these indirect routes. Previous studies have addressed the synthesis of catalysts with improved C_2 yields and selectivities where $Mn/Na_2WO_4/SiO_2$ catalysts[4−7] have achieved among the highest reported C_{2+} yields 26%.[2,8]

OCM reactions involve the catalytic formation of methyl groups,[9,10] which desorb as free radicals ($CH_3^{\bullet}$) that ultimately react via predominantly homogeneous pathways. Recombination of CH_3 radicals in the gas phase forms C_2H_6 and subsequent dehydrogenation steps convert C_2H_6 to C_2H_4.[11] CO_x (CO and CO_2) forms via catalytic and homogeneous primary and secondary pathways. Homogeneous pathways can also form C_{3+} hydrocarbons, which contain weaker C−H bonds that favor their subsequent conversion to CO_x.[12,13] Selectivities and yields depend on the identity and dynamics of specific elementary steps involved in these primary and secondary reactions. The details of such kinetic networks remain incomplete; yet, they are essential to describe these reactions in terms of their rate constants and pressure dependences and to define and exploit the specific contributions and kinetic coupling of surface-catalyzed and gas phase reactions.

SCHEME 1: Reaction Pathway for Oxidative Coupling of Methane

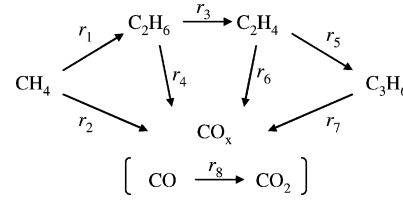

C_2 selectivities typically decrease as CH_4 conversion increases because primary C_2 products oxidize to CO_x products favored by thermodynamics. Such sequential pathways (Scheme 1) account for the inherently limited yield of OCM processes.[12−16] CH_4 reacts first to form C_2H_6 and undesired CO_x byproducts via surface-catalyzed and homogeneous pathways, the rates of which depend on the relevant rate constants (k_1, k_2; Scheme 1), the reactant pressures (CH_4, O_2), and the concentration of

* Corresponding author. Tel: 1-510-642-9673. Fax: 1-510-642-4778. E-mail: iglesia@berkeley.edu.

[†] Current address: Department of Chemical System Engineering, The University of Tokyo, 7-3-1 Hongo Bunkyoku, Tokyo, 113-8656 Japan.

10.1021/jp9001302 CCC: $40.75
Published on Web 05/13/2009

reaction products (C_2H_6, C_2H_4, CO_x, H_2O) prevalent at conversions required for practical OCM applications. C_2 products are favored by high CH_3 radical concentrations because their recombination is a bimolecular event, while competing oxidation pathways are proportional to CH_3 concentration because they involve reactions with O_2-derived species. CH_3 oxidation depends on O_2 concentrations, while CH_3 recombination rates are independent of O_2 pressure. Attainable C_{2+} yields depend sensitively on the relative rates of secondary reactions of C_2 and C_{3+} products (r_3-r_7; Scheme 1) and of primary CH_4 activation steps (r_1). These secondary reactions involve the activation of C−H bonds to form the various radical intermediates (C_2H_5, C_2H_3, etc.) via homolytic pathways similar in nature to those involved in CH_4 activation.[9,11] As a result, the relative rates of these reactions and the concomitant attainable maximum C_2 yields are essentially dictated by the relative C−H bond energies among the hydrocarbons involved in OCM.[17]

We report here rigorous kinetic and isotopic assessments of primary and secondary OCM pathways and their elementary steps. We also provide evidence for previously unrecognized effects of H_2O on the relative rates of these steps and confirm the kinetic irrelevance of the other OCM products (C_2H_6, C_2H_4, CO_x) in C−H bond activation of CH_4 reactants. Specifically, we show that H_2O-derived gas phase OH radicals activate C−H bonds in CH_4 and C_2H_6 with less sensitivity to their respective C−H bonds energies. We also find that the preponderance of OH-mediated homogeneous pathways (via intervening surface activation of H_2O) ameliorates C_2H_4 combustion routes favored by the preferential binding of alkenes (C_2H_4, C_3H_6) on oxide surfaces. As a result, these OH-mediated pathways lead to higher C_2 selectivities and yields than are attainable with anhydrous reactants. These data, taken together with simulations using rigorous kinetic models, provide evidence for the relevance and consequences of quasi-equilibrated surface-catalyzed formation of reactive OH radicals from O_2-H_2O reactants. The resulting OH-mediated pathways become the predominant route for OCM reactions as conversion increases or as H_2O is added to CH_4-O_2 reactant streams; these pathways lead to limiting yields higher than C−H activation routes that prevail under anhydrous conditions and are mediated exclusively by surface oxygen species at catalytic surfaces.

We have reported preliminary evidence for these selectivity improvements from OH-mediated pathways in a previous short communication.[18] The formation of OH radicals from O_2-H_2O mixtures has also been detected on basic oxides (e.g., La_2O_3, Nd_2O_3),[19,20] apparently on the same sites that activate C−H bonds, a conclusion reached from the observed inhibition of OH formation by reactions of CH_4.[21] These studies have also suggested that OH radicals would increase OCM rates, without experimental evidence, by activating C−H bonds through homogeneous pathways, but also concluded that such pathways would not influence C_2 selectivities or yields, because OH radicals would activate C−H bonds in CH_4 and OCM products with similar specificity.[20] Two patents have disclosed positive effects of H_2O on CH_4 conversion rates and C_2 selectivities on supported Mn-based catalysts,[22,23] without mechanistic elucidation or speculation, and without any evidence for rigorous kinetic control or specific chemical effects of H_2O (instead of concomitant and unintended changes in mass or heat transfer rates).

We show here that OH radicals react with C−H bonds with less sensitivity to the C−H bond strengths in CH_4 and C_2H_6 than surface oxygens and with much lower reactivity for C_2H_4 than routes mediated by surfaces. Rate constants for surface-mediated pathways, measured under H_2O-free conditions, predict C_2 yields much lower than attained in practice, illustrating the essential role of OH-mediated pathways, even without intentional addition of H_2O to CH_4-O_2 reactants. In contrast, kinetic models that embed both surface-catalyzed and OH-mediated steps and their rate constants accurately describe measured C_2 synthesis rates, yields, and selectivities. We report the kinetic effects of O_2 pressure on OCM rates, selectivities, and yields and their implications for staged O_2 injection strategies[15,24] that aim to maintain low O_2 pressures while providing stoichiometric amounts of O_2. Such strategies become effective in improving C_2 yields only when C_2 oxidation rates (r_4, r_6, r_7) are more sensitive to O_2 pressure than CH_4 activation rates (r_1). We find that O_2 pressure effects are similar for activation of reactants (CH_4) and products (C_2H_6, C_2H_4); thus, staging and membrane[25] strategies are unlikely to improve C_2 yields, but may be useful to control local exotherms or to extract O_2 from air during OCM. The concepts reported here, as well as their catalytic consequences, are applicable in general to attain high OCM yields.

2. Experimental Section

Catalysts were prepared using procedures reported previously.[6] SiO_2 (Davison Chemicals, Silica Gel grade 57) was sieved to retain aggregates 0.10−0.85 mm in diameter. These aggregates were contacted with aqueous $Mn(NO_3)_2$ solutions (50 wt %; Strem Chemicals, 2 cm^3/g-SiO_2) for 2 h and treated in ambient air at 403 K for 5 h.[6] The samples were then stirred in an aqueous solution of $Na_2WO_4 \cdot 2H_2O$ (Sigma-Aldrich, 99%, 2 cm^3/g-SiO_2) to give 2 wt % Mn and 5 wt % Na_2WO_4. Finally, the samples were treated in ambient air at 403 K for 5 h and in flowing dry air (Praxair, UHP, 10 g-cat, 0.167 cm^3 s^{-1}) by increasing the temperature at 0.033 K s^{-1} and holding at 1173 K for 8 h. The samples were sieved again before use to retain aggregates with a narrower size range (0.25−0.35 mm).

OCM rates and selectivities were measured in flow and recirculating batch reactors using U-shaped quartz reactor cells (4 mm I.D.). Catalysts (0.02−0.05 g) were diluted with inert SiO_2 particles (0.5 g; Fluka, 0.25−0.35 mm) and held onto quartz wool. The temperature was controlled using a Watlow controller (Series 982) and a resistively heated furnace and was measured with a K-type thermocouple contacting the outer surface of the reactor. CH_4 (Praxair, 99.999%) and O_2 (Praxair, 99.999%) were introduced with He (Praxair, 99.999%) as a diluent using mass flow controllers (Porter Inc. model 201). In batch experiments, the recirculation volume (275−650 cm^3) was evacuated to <0.1 Pa before introducing reactants, which were continuously circulated using a graphite gear pump (Micropump, model 182-000, >2.5 cm^3 s^{-1}). Water was removed as it was formed in some experiments using a dry ice/acetone cold trap held within the recirculating line. Reactant and product concentrations were measured with a HP5890 gas chromatograph using a Carbosieve SII packed column (Supelco, 3.2 mm × 2 m) with a thermal conductivity detector and a HP-PLOT Q capillary column (Agilent Technology Inc., 0.32 mm × 30 m) with a flame ionization detector. Differential rates were obtained from time-derivatives of hydrocarbon concentration profiles in batch reactors, after regressing concentration−time data to a sixth-order polynomial. Selectivities and yields are reported on a carbon basis as cumulative integral values.

CD_4 (Isotec, 99 at % D), D_2O (Cambridge Isotope Laboratories, Inc., 99.9%), and $^{18}O_2$ (Isotec, 99 at % ^{18}O) were used to measure kinetic isotope effects and isotopic scrambling dynamics. Isotopic tracer studies were carried out using labeled $^{13}CH_4$ (Isotec, 99 at % ^{13}C) in the presence of $^{12}C_2H_6$ (Praxair, chemical purity 99.999%), $^{12}C_2H_4$ (Praxair, chemical purity

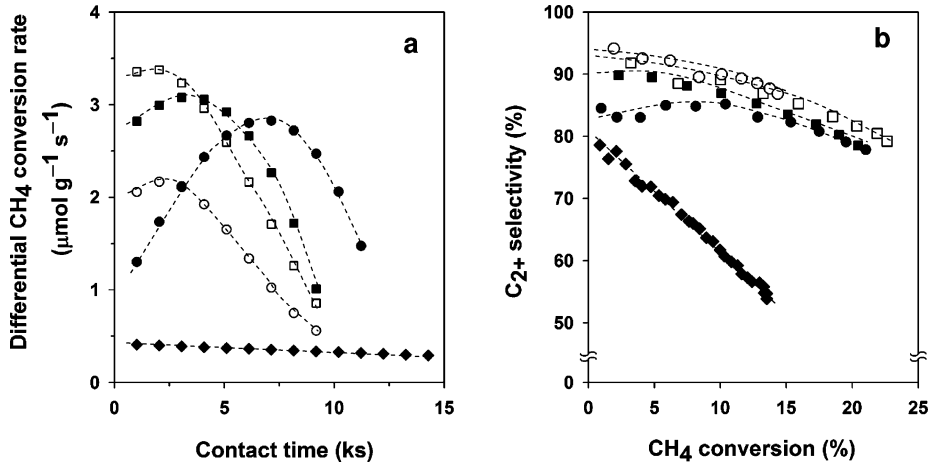

Figure 1. Differential CH_4 conversion rate as a function of contact time (a) and C_{2+} selectivity as a function of CH_4 conversion (b) measured in a recirculating reactor (0.02 g, 1073 K, volume: 275−650 cm^3, 10.7 kPa CH_4, 101 kPa total pressure, balance He, (◆) 1.8 kPa O_2, H_2O removed;[18] (●) 1.8 kPa O_2, steady state reaction;[18] (■) 1.8 kPa O_2, 0.4 kPa H_2O added;[18] (□) 1.8 kPa O_2, 0.9 kPa H_2O added; (○) 0.9 kPa O_2, 0.4 kPa H_2O added).

99.999%), or 5% $^{12}C_3H_6$/He (Praxair). Labeled ^{13}CO (Isotec, 99% ^{13}C) was used to measure CO oxidation rates during OCM. These isotopic studies used the gas chromatograph described above and also a HP5890 GC equipped with a mass selective detector (HP 5972) connected to a HP-PLOT Q capillary column.

Simulations were carried out using ChemKin codes[26] and reported gas-phase rate constants and thermodynamics.[14] This homogeneous kinetic model contains 447 reversible elementary chemical reactions and 115 species.

The surface area of the $Mn/Na_2WO_4/SiO_2$ sample, after treatment in dry flowing air at 1173 K for 8 h, was 1.3 $m^2\ g^{-1}$, as determined from N_2 physisorption at its normal boiling point using the BET formalism.[27] This treatment sinters samples to an extent that renders them stable against further changes in structure or surface area during subsequent catalytic tests, as reported earlier.[7] No detectable changes in OCM rates or selectivities were detected for >80 ks after such thermal treatments.

3. Results and Discussion

3.1. Effects of H_2O Pressure on CH_4 Conversion Rates and C_{2+} Selectivity. Figure 1, panels a and b, shows differential CH_4 conversion rates per gram of catalyst; from time derivatives of concentration profiles as a function of contact time and C_{2+} selectivities as a function of CH_4 conversion, respectively, on $Mn/Na_2WO_4/SiO_2$ catalysts in a gradientless batch reactor at 1073 K. At 10.7 kPa CH_4 and 1.8 kPa O_2 (filled circles; "steady state reaction"), Figure 1a shows that CH_4 conversion rates initially increased with contact time and then decreased as O_2 coreactants were depleted in all experiments for which reactants and products were kept in contact with the catalyst. C_2 selectivities remained nearly constant up to ~10% CH_4 conversion and subsequently decreased gradually as conversion increased with contact time (Figure 1b).

This enhancement in CH_4 conversion rate with increasing conversion (and contact time) was not caused by local high temperatures as a result of exothermic CH_4 oxidation reactions,[7] because varying catalyst dilution with quartz particles (0:1 to 50:1 quartz to catalyst ratio) did not detectably influence measured rates. The recirculation strategy used here minimizes the amount of energy released per pass compared with commonly used single-pass flow reactors.[28,29] Changes in catalyst structure or accessibility also do not account for the observed increase in rates, because these trends were observed again when reactor contents were replaced with fresh CH_4/O_2 reactants directly after one of these experiments and without intervening thermal treatments. We conclude, therefore, that these "activation" or "autocatalytic" trends are kinetic in origin; they must reflect either a negative kinetic order in CH_4 or O_2 reactants, which are depleted with contact time, or positive effects by one or more of the OCM products (C_2H_6, C_2H_4, CO, CO_2, and H_2O), which increase in concentration as conversion increases with contact time.

We observe in independent experiments an increase in CH_4 conversion rate with increasing CH_4 and O_2 pressures in the initial reactant stream. We do not find, however, any detectable effects of ethene or ethane on rates or selectivities (vide infra). Thus, negative kinetic orders in reactants or positive effects of C_2 products cannot account for the observed increase in CH_4 conversion rates with contact time. As we have shown earlier,[18] H_2O may instead affect CH_4 reactions, consistent with the data in Figure 1, panels a and b, in which H_2O was either continuously removed as it formed in OCM reactions (labeled "H_2O removed") or added to the initial reactant mixtures (labeled "H_2O added").

The continuous removal of H_2O during OCM reactions led to CH_4 conversion rates that decreased monotonically with increasing contact time and CH_4 conversion, as expected from the gradual depletion of reactants and the positive OCM kinetic orders in CH_4 and O_2 pressures (filled diamonds; Figure 1a). C_2 selectivities decreased with contact time more strongly when H_2O was removed than when it was allowed to accumulate during reaction or when it was added initially together with reactants (Figure 1b). H_2O addition (0.4 kPa) to CH_4-O_2 reactants led to higher initial CH_4 conversion rates than for anhydrous reactants and to a subsequent decrease in rates as reactants were depleted (filled squares; Figure 1a). Higher H_2O pressures (0.9 kPa) led to even higher initial rates (open squares; Figure 1a). H_2O addition also increased initial C_2 selectivities (Figure 1b). These effects of water became weaker as CH_4 conversion increased, because H_2O concentrations increased to similar levels as conversion increased, even with anhydrous feeds.

An earlier study proposed that OH radicals formed from H_2O could increase CH_4 activation rates, but not C_2 selectivities,

during OCM reactions.[20] Our results show that H_2O markedly influences both rates and selectivities. These effects are discussed next in the context of the kinetic response of the various steps to CH_4 and O_2 pressures in the absence of H_2O. We then address the specific effects of H_2O in the steps required for the activation of CH_4, C_2H_6, and C_2H_4 (Scheme 1) and report rate constants for surface-mediated and H_2O-mediated reaction pathways using isotopic tracing methods. We also report kinetic isotope effects and scrambling rates that probe the nature and reversibility of the relevant elementary steps.

3.2. Rate Equations and Elementary Steps for CH_4/O_2 Reactions under Anhydrous Conditions. The kinetic response of CH_4 conversion rates to CH_4 and O_2 pressures was measured on $Mn/Na_2WO_4/SiO_2$ at 1073 K in a plug-flow reactor by varying space velocity and inlet concentrations. Rates and selectivities were extrapolated to zero CH_4 conversion to measure kinetic data under strictly anhydrous conditions (using five data points at CH_4 conversions below 5%). No reaction products were detected in the absence of a catalyst at these reaction conditions.

Measured CH_4 conversion rates (r_{CH_4}) were proportional to $P_{CH_4}P_{O_2}^{1/2}$, as previously reported;[6] these data are consistent with quasi-equilibrated dissociative O_2 chemisorption on vicinal surface vacancies (*) to form reactive O_s* species (step 1) and with kinetically-relevant steps in which these O_s* species abstract H-atoms from CH_4 to form adsorbed OH* and gas-phase methyl radicals (step 2). This catalytic sequence is then completed via quasi-equilibrated recombination of OH* to form H_2O and surface vacancies (step 3):

$$O_2 + 2* \overset{K_{O_2}}{\rightleftharpoons} 2O_s* \quad (1)$$

$$CH_4 + O_s* \xrightarrow{k'_{CH_4}} CH_3\cdot + OH* \quad (2)$$

$$2OH* \rightleftharpoons H_2O + O_s* + * \quad (3)$$

Kinetic data cannot be used to determine whether H-abstraction occurs from gas phase CH_4 or from CH_4 weakly adsorbed at low coverages in step 2, because both predict rates proportional to CH_4 pressure. These steps and the pseudosteady state assumption for all adsorbed species lead to CH_4 conversion rates given by

$$r_{CH_4} = k'_{CH_4}P_{CH_4}\frac{\sqrt{K_{O_2}P_{O_2}}}{1+\sqrt{K_{O_2}P_{O_2}}} \quad (4)$$

at conditions where products are present at low concentrations and their kinetic effects are negligible. Figure 2 shows (P_{CH_4}/r_{CH_4}) ratios as a function of $P_{O_2}^{1/2}$. The identical linear correlations at these two CH_4 partial pressures are consistent with eq 4. The value of K_{O_2} obtained from these data was very small (0.005 ± 0.01 kPa^{-1}), indicating that O_s* coverages are very small during OCM catalysis. Hence, eq 4 becomes

$$r_{CH_4} = k'_{CH_4}K_{O_2}^{1/2}P_{CH_4}P_{O_2}^{1/2} \quad (5)$$

The small K_{O_2} value reflects the weakly bound nature of active oxygen species (e.g., O^- or O_2^{2-} species[9,31]).

The temperature dependence of CH_4 conversion rate constants under anhydrous conditions ($k' = k'_{CH_4}K_{O_2}^{1/2}$ in Figure 3; 993−1123 K) gives an apparent activation energy (E_{app}) of 290 ± 8 kJ mol^{-1}, consistent with previously reported values (280 kJ mol^{-1}).[6] This activation energy reflects the combined contributions from the activation barrier for H-abstraction in step 2 ($E_{a,O*}$) and the enthalpy for dissociative O_2 adsorption in step 1 (ΔH_{O_2})

$$E'_{app} = E_{a,O*} + \frac{1}{2}\Delta H_{O_2} \quad (6)$$

If O_2(g) loses all degrees of freedom upon adsorption to form O_s* (step 1), the measured K_{O_2} (0.005 kPa^{-1} at 1073 K) corresponds to a ΔH_{O_2} value of −176 kJ mol^{-1}. Equation 6 and measured E_{app} values (290 ± 8 kJ mol^{-1}) then give an activation energy for step 2 ($E_{a,O*}$) of 378 kJ mol^{-1}. This energy is similar to that required to dissociate C−H bonds in CH_4 (439 kJ mol^{-1})[32] without any concerted interactions with surfaces or other molecules; it is indicative of a late transition state along the reaction coordinate. In practice, O_s* is expected to retain some translational freedom (leading to weaker M-O bonds and less negative ΔH_{O_2}values), because the strength of O_s* binding allow some surface migration at typical OCM reaction temperatures. O_2 adsorption processes, however, must be exothermic

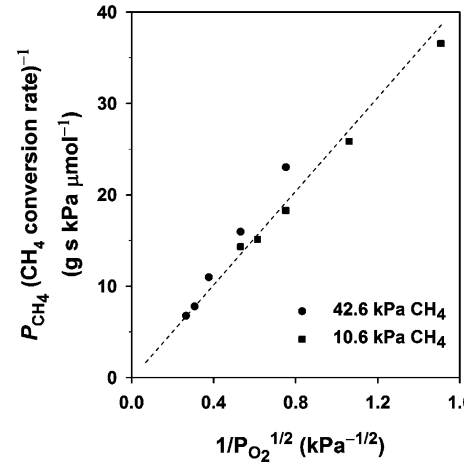

Figure 2. Effects of O_2 partial pressure on CH_4 conversion rate. The rates are divided by CH_4 partial pressure and the reciprocal plots are shown. All rates are taken by extrapolation to zero conversion from the results at varied conversions (0.05 g, 1073 K, 101 kPa total pressure, balance He).

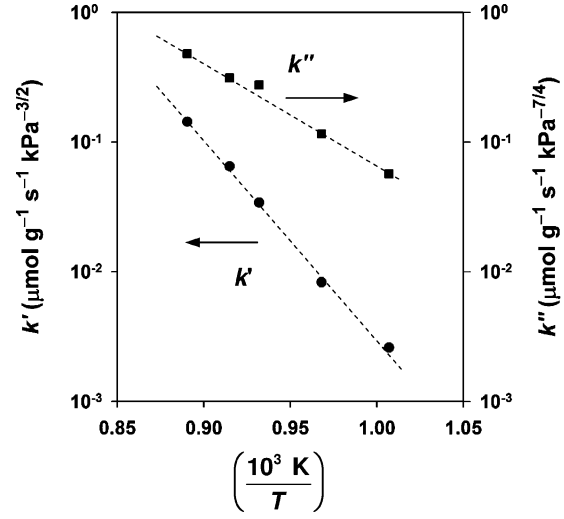

Figure 3. Arrhenius plots for rate constants in the rate expression: $r_{CH_4} = k'P_{CH_4}P_{O_2}^{1/2} + k''P_{CH_4}P_{O_2}^{1/4}P_{H_2O}^{1/2}$ (eq 19) (0.02 g, 1073 K, volume: 550 cm^3, 10.7 kPa CH_4, 1.8 kPa O_2, 101 kPa total pressure, balance He).

TABLE 1: Kinetic Isotope Effects Measured in a Recirculating Reactor (0.02 g, 1073 K, Unit Volume 550 cm^3, 10.7 kPa CH_4 or CD_4, 0.4 kPa H_2O or D_2O (when Added), 101 kPa Total Pressure, Balance He)

rate ratio	O_2 (kPa)	KIE
CH_4-O_2/CD_4-O_2	3.5	1.29
CH_4-O_2/CD_4-O_2	1.8	1.25
CH_4-O_2/CD_4-O_2	0.9	1.24
$(CH_4-O_2-H_2O)/(CD_4-O_2-H_2O)$	1.8	1.44
$[(CH_4-O_2-H_2O) - (CH_4-O_2)]/[(CD_4-O_2-H_2O) - (CD_4-O_2)]$	1.8	1.58
$CH_4-O_2-H_2O/CH_4-O_2-D_2O$	1.8	1.08

for them to occur, because of the concomitant entropy losses upon adsorption. Therefore, intrinsic C−H bond activation barriers must be larger than those measured (>290 kJ mol^{-1}). These data seem to indicate that the role of O_s* is predominantly to scavenge H atoms by forming OH* and that its role in stabilizing late transition states with significant radical character in the CH_3 moiety is relatively small.

We have probed the kinetic relevance of C−H bond activation steps by measuring kinetic isotope effects (KIE) for CH_4/O_2 and CD_4/O_2 reactants (Table 1). Rates were measured by extrapolation to zero conversion to ensure anhydrous conditions. Normal KIE values (1.24−1.29, Table 1) were found at all O_2 pressures (0.9−3.5 kPa), consistent with C−H bond activation as the kinetically relevant step, as discussed in more detail in the Supporting Information.

The extent to which C−H bond activation steps are reversible during OCM reactions was determined from the rate of formation of mixed $CH_xD_{(4-x)}$ ($0 < x < 4$) isotopomers (here used to denote molecules with different x values) during reactions of $CH_4/CD_4/O_2$ isotopic mixtures. The ratio of the isotopic scrambling rate to the chemical conversion rate was negligible (≪1) (Figure 4); these data show that C−H bond activation steps (step 2) are essentially irreversible during OCM reactions. $CH_xD_{(4-x)}$ isotopomers gradually formed with increasing contact time and CH_4 conversion as a result of homogeneous H-transfer reactions between $CH_3^\bullet$ and CH_4 (or C_2H_6) (e.g., $CH_3^\bullet + C_2H_6 \rightarrow CH_4 + C_2H_5^\bullet$).

The quasi-equilibrated nature of O_2 dissociation steps (step 1) was confirmed from the rate of isotopic scrambling in dioxygen molecules during reactions of $CH_4/^{16}O_2/^{18}O_2$ mixtures

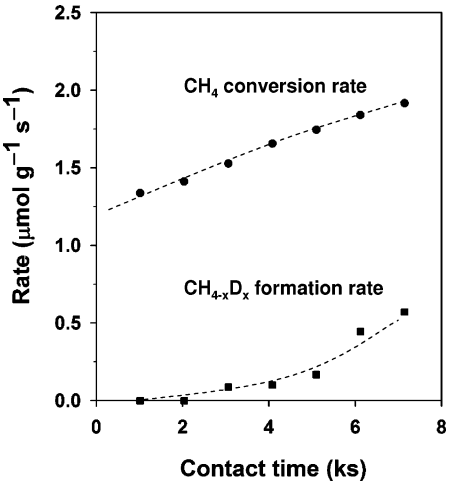

Figure 4. Methane chemical conversion and CH_4/CD_4 cross exchange rates during reaction of $CH_4/CD_4/O_2$ mixture measured in a recirculating batch reactor (0.02 g, 1073 K, volume: 550 cm^3, 5.3 kPa CH_4 and CD_4, 1.8 kPa O_2, 101 kPa total pressure, balance He).

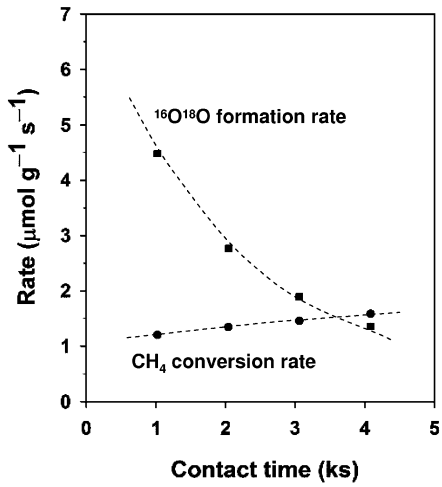

Figure 5. Methane chemical conversion rate and $^{16}O^{18}O$ isotopomer formation rate during the reaction of $CH_4/^{16}O_2/^{18}O_2$ mixture measured in a recirculating batch reactor (0.02 g, 1073 K, volume 550 cm^3, 10.7 kPa CH_4, 0.9 kPa $^{16}O_2$, 0.9 kPa $^{18}O_2$, 101 kPa total pressure, balance He).

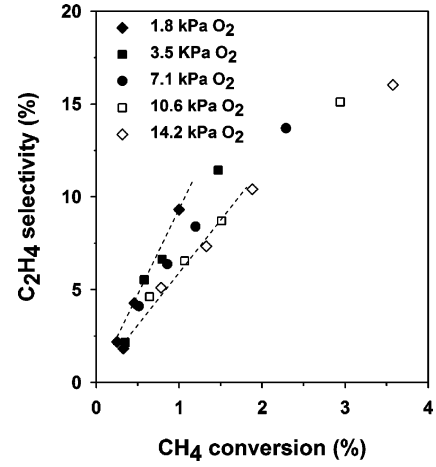

Figure 6. C_2H_4 selectivity as a function of CH_4 conversion measured in a flow reactor (0.05 g, 1073 K, CH_4 42.6 kPa, 101 kPa total pressure, balance He, 1.0−2.5 cm^3 s^{-1} total flow rate). Dashed lines denote linear regressions of the results at low CH_4 conversions (<2%) for data of 1.8 and 14.2 kPa O_2.

(Figure 5). Rates extrapolated to zero conversion were ∼10 times larger for $^{16}O^{18}O$ isotopomers (via the reverse of step 1) than for CH_4 chemical conversion (step 2). These data are consistent with fast and quasi-equilibrated O_2 dissociation (eq 1). We note, however, that these relative rates differ by only a factor of ∼10 and that the assumption of quasi-equilibrium may become inaccurate as CH_4 pressure increases or O_2 pressure decreases by commensurate factors, because these two molecules determine the rates at which O_s* species react and form, respectively. The breakdown of the quasi-equilibrium assumption for O_2 chemisorption as O_2 is depleted with increasing conversion is addressed later (section 3.4).

3.3. Effects of Reactant Concentrations on OCM Selectivity under Anhydrous Conditions. We examine next product formation rates and selectivities from CH_3 radicals, the species involved intermediates in OCM reactions and formed in step 2,[9,10] under anhydrous conditions. First, we examine whether C_2H_4 can be formed directly from CH_4/O_2 mixtures on Mn/Na_2WO_4/SiO_2 at 1073 K. Figure 6 shows C_2H_4 selectivities as a function of CH_4 conversion at several O_2 pressures (1.8−14.2 kPa; 42.6 kPa CH_4). Initial C_2H_4 selectivities (at zero conversion)

are essentially zero, indicating that ethene forms only via dehydrogenation of primary C_2H_6 products, instead of directly from CH_4 (or CH_3 radicals). These data contradict previous proposals that C_2H_4 can form directly from CH_4 via carbene intermediates.[33] Very low conversions (<1%) are essential to probe the identity of primary and secondary products because of the strong effects of H_2O on OCM rates and C_2 selectivities as CH_4 conversion increases with residence time. Our rigorous extrapolation to low conversions shows unequivocally that C_2H_6, CO and CO_2 are the only primary products formed from CH_4/O_2 reactants.

Figure 7a−c shows C_2H_6, CO, and CO_2 formation rates (extrapolated to zero conversion) as a function of CH_4 pressure in a flow reactor. These rates rigorously reflect the formation of each product directly from CH_4/O_2 reactants. CH_3 radicals recombine to form C_2H_6 (step 7), but may also react to give CO and CO_2; CO_x also shows selectivity trends with residence time consistent with primary products, even though they form via $CH_3^{\bullet}$, because these $CH_3^{\bullet}$ reactive intermediates are very reactive during OCM reactions and are present at their pseudosteady-state concentrations. Panels b and c in Figure 7 (and data from O_2 pressure variations shown in Figure S1 in the Supporting Information) show that O_2 pressures influence CO formation rates more strongly than CO_2 formation rates, suggesting that CO_2 forms predominantly via reactions of $CH_3^{\bullet}$ with O* ($\sim P_{O_2}^{1/2}$), either before or after CH_3 desorption, while CO forms predominantly via $CH_3^{\bullet}$ reactions with gas-phase O_2 ($\sim P_{O_2}$). These findings are consistent with the sequence

$$2CH_3^{\bullet} + M \xrightarrow{k_{C_2}} C_2H_6 + M \quad (7)$$

$$CH_3^{\bullet} + O_2 \xrightarrow{k_{CO}} CO \quad (8)$$

$$CH_3^{\bullet} + O^* \xrightarrow{k_{CO_2}} CO_2 \quad (9)$$

in which M denotes a "third-body" that dissipates the energy released by radical recombination. These elementary steps and the assumptions of pseudosteady-state CH_3 concentrations, quasi-equilibrated O_2 dissociation, and low O_s* coverages lead to rate equations of the form

$$r_{C_2} = k_{C_2} P_{CH_3}^{\ 2} \quad (10)$$

$$r_{CO} = k_{CO} P_{CH_3} P_{O_2} \quad (11)$$

$$r_{CO_2} = k_{CO_2} P_{CH_3} P_{O_2}^{1/2} \quad (12)$$

$$P_{CH_3} = \frac{\sqrt{B^2 + 4k_{C_2} k' P_{CH_4} P_{O_2}^{1/2}} - B}{2k_{C_2}} \quad (\text{where } B = k_{CO} P_{O_2} + k_{CO_2} P_{O_2}^{1/2}) \quad (13)$$

Regressed rate constants[34] were obtained from rates measured as a function of CH_4 and O_2 pressures (data from Figure 2, panels a and b). The curves drawn in Figure 7a−c illustrate the accuracy of these kinetic descriptions of OCM pathways. The effects of CH_4 and O_2 pressures on C_2 selectivities are given by eq 14, which is derived from eqs 5 and 10−13, together with the regressed values of their respective rate constants

$$\frac{r_{C2}}{r_{CO} + r_{CO_2}} = \frac{1}{2}\left(\sqrt{1 + \frac{4k' k_{C_2} P_{CH_4}}{(k_{CO} P_{O_2}^{1/2} + k_{CO_2})^2 P_{O_2}^{1/2}}} - 1\right) \quad (14)$$

At high selectivity ratios (∼>4), eq 14 can be simplified to

$$\frac{r_{C2}}{r_{CO} + r_{CO_2}} = \sqrt{\frac{k' k_{C_2} P_{CH_4}}{(k_{CO} P_{O_2}^{1/2} + k_{CO_2})^2 P_{O_2}^{1/2}}} \quad (15)$$

because the $(4k'k_{C_2}P_{CH_4})/[(k_{CO}P_{O_2}^{1/2} + k_{CO_2})^2 P_{O_2}^{1/2}]$ term is much larger than unity. This ratio increases with increasing CH_4 pressure and decreasing O_2 pressure (and thus with increasing CH_4/O_2 ratio) and also as surfaces become more reactive for CH_4 activation to form CH_3 radicals (larger k'). The k'_{C-H}/k'_{C-D} ratio obtained for CH_4 and CD_4 reactants (1.25; Table 1) and its use in eq 15 indicates that C_2 selectivities at a give methane to oxygen reactant ratio ($\sim\{(k'k_{C_2})/(k_{CO}P_{O_2}^{1/2} + k_{CO_2})^2\}^{1/2}$) would be ∼2% lower for CD_4-O_2 than for CH_4-O_2 reactions. Measured selectivities are almost identical for CH_4 and CD_4 at each O_2 pressure (∼94%, ∼82%, and ∼78% selectivities at 0.9, 1.8, and 3.5 kPa O_2, respectively). These similar selectivities may arise from positive but small isotope effects for k_{CO} and k_{CO_2}, which reflect H-abstraction from methyl radicals and which cancel those for the numerator ($k'k_{C_2}$) in eq 15. We note that the form of eq 15 accurately describes primary selectivities in anhydrous mixtures and that these selectivities depend predominantly on CH_4/O_2 reactant ratios.

3.4. H_2O-Mediated C−H Bond Activation Pathways. We examine next the mechanistic basis for the strong effects of H_2O on CH_4 conversion rates and C_{2+} selectivities and yields (Figures 1a and 1b). The activation of C−H bonds in hydrocarbons by H_2O without O_2 co-reactants was probed using $CH_4/H_2O/C_2H_6$ (or C_2H_4) reactants at 1073 K in a recirculating batch reactor. CO and CO_2 were not detected at any conditions, indicating that steam reforming reactions of CH_4, C_2H_6, or C_2H_4 did not occur. These data also show that any prevalent H_2O-mediated pathways require O_2-derived O* species on catalytic surfaces for OH formation.

Laser-induced fluorescence was previously used to detect OH radicals when H_2O/O_2 mixtures were exposed to solid basic oxides that also catalyze OCM reactions.[19−21] The presence of CH_4 decreased OH concentrations present in H_2O/O_2 mixtures, suggesting that CH_4 and H_2O scavenge similar active oxygens at surfaces (O_s*).[21] Thus, we conclude that OH radicals form via the coupling of step 3 with

$$H_2O + O_s^* \rightleftarrows OH^{\bullet} + OH^* \quad (16)$$

in which $OH^{\bullet}$ and OH* denote radical and chemisorbed species, respectively. Previous studies[20] have shown that OH radicals reach equilibrium concentrations on La_2O_3 solids (100 Pa H_2O and O_2; 1173 K) via

$$O_2 + 2H_2O \overset{K_{OH^{\bullet}}}{\rightleftarrows} 4OH^{\bullet} \quad (17)$$

as a consequence of equilibrated steps 1, 3, and 16. OH radicals thus formed can subsequently abstract H atoms from CH_4 via homogeneous pathways

$$CH_4 + OH^{\bullet} \xrightarrow{k''_{CH_4-OH^{\bullet}}} CH_3^{\bullet} + H_2O \qquad (18)$$

This reaction is exothermic by 59 kJ mol^{-1} at 1073 K.[35] When OH radicals are at equilibrium (via step 17), the rate of C−H activation (via step 18) becomes proportional to $P_{O_2}^{1/4}P_{H_2O}^{1/2}$. The combined rates of CH_4 reactions via surface O_s*-mediated and OH-mediated H-abstractions are then given by

$$r_{CH_4} = k'P_{CH_4}P_{O_2}^{1/2} + k''P_{CH_4}P_{O_2}^{1/4}P_{H_2O}^{1/2} \qquad (19)$$

where k'' is given by $k''_{CH_4-OH^{\bullet}}K_{OH^{\bullet}}^{1/4}$, $k''_{CH_4-OH^{\bullet}}$ is the rate constant for step 18, and P_{O_2} is the equilibrium constant for step 17. H_2O pressures were determined at each point by an oxygen balance on reactants and products. Figure 8a shows that incremental CH_4 conversion rates introduced by H_2O-mediated pathways (the difference between rates with and without H_2O

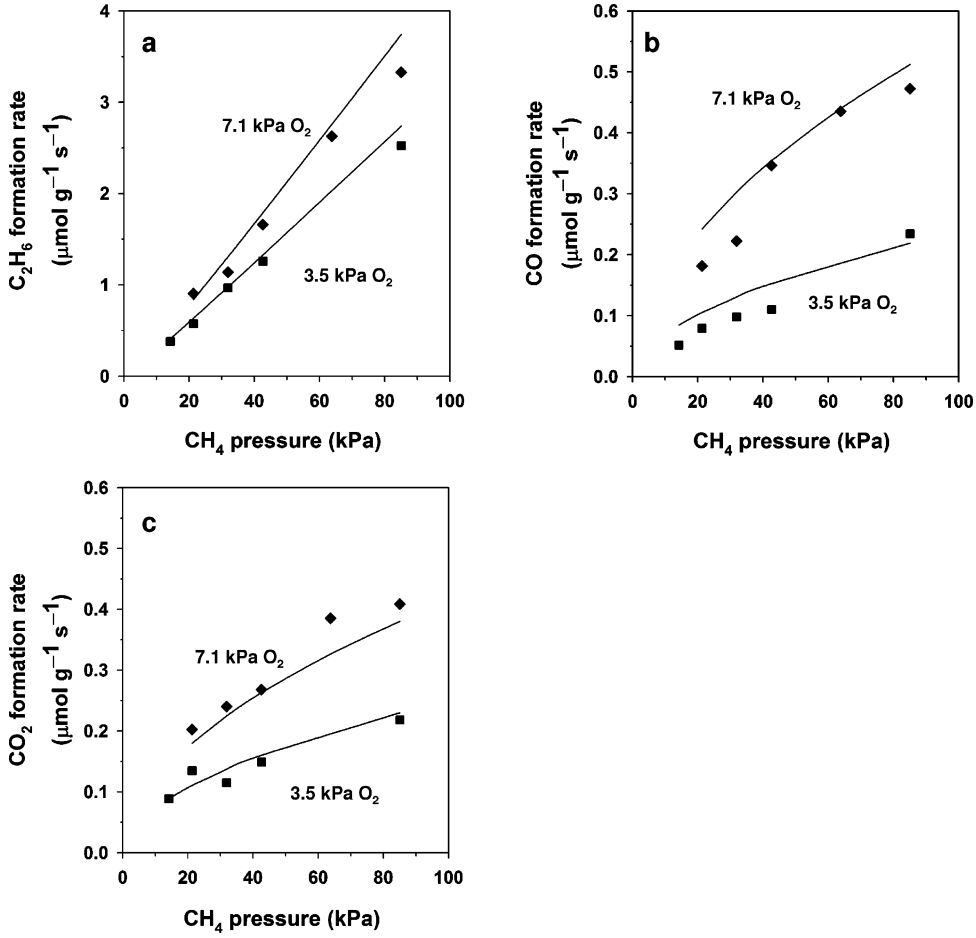

Figure 7. C_2H_6 (a), CO (b), and CO_2 (c) formation rates extrapolated to zero conversion as a function of CH_4 pressure measured in a flow reactor (0.05 g, 1073 K, 101 kPa total pressure, balance He). The curves denote the fitting results using optimized rate constants (eqs 10−13).

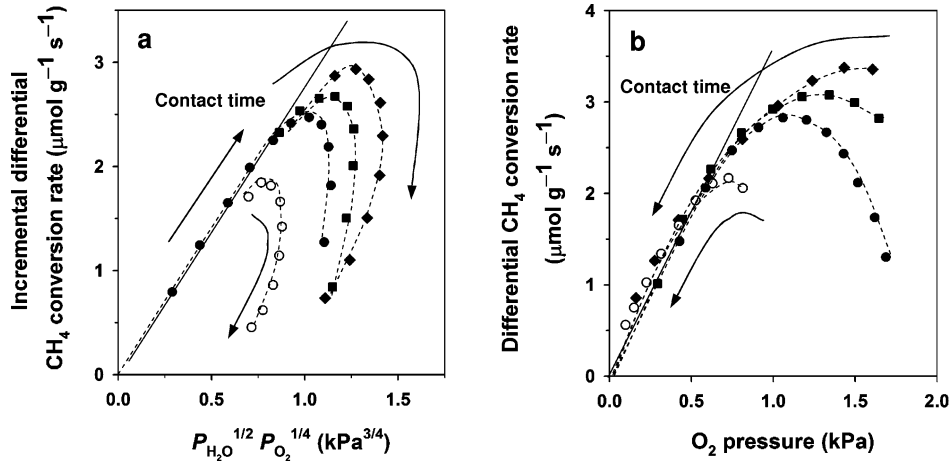

Figure 8. Incremental differential CH_4 conversion rate (from measured differences between rates with and without H_2O) as a function of $P_{O_2}^{1/4}P_{H_2O}^{1/2}$ (a) and (total) CH_4 conversion differential rate as a function of O_2 pressure (b) measured in a recirculating batch reactor. The arrows are in the direction of increasing contact time (0.02 g, 1073 K, volume: 275−650 cm^3, 10.7 kPa CH_4, 101 kPa total pressure, balance He, (●) 1.8 kPa O_2; (■) 1.8 kPa O_2, 0.4 kPa H_2O added; (□) 1.8 kPa O_2, 0.9 kPa H_2O added, (○) 0.9 kPa O_2, 0.4 kPa H_2O added).

and given by the second term in eq 19) are proportional to $P_{O_2}^{1/4}P_{H_2O}^{1/2}$ at low conversions (short contact times), consistent with quasi-equilibrated OH$^\bullet$ formation steps (step 17) and with the kinetic relevance of OH-mediated H abstraction (step 18). The rate constants for OH-mediated H abstraction (k''; 0.21 μmol g^{-1} s^{-1} kPa$^{-7/4}$) and surface-mediated H abstraction (k'; 0.04 μmol g^{-1} s^{-1} kPa$^{-3/2}$) at 1073 K give corresponding rates of 1.7 and 0.7 μmol g^{-1} s^{-1} for the two terms in eq 15 at 0.4 kPa H_2O (10.7 kPa CH_4; 1.8 kPa O_2), indicating the significant contributions from OH-mediated pathways at typical OCM conditions.

Figure 8a shows that differential CH_4 conversion rates decrease abruptly at longer contact times, as O_2 is essentially depleted from the reactant stream. These trends reflect a decrease in the rate of O_2 chemisorption and an increase in the rate of scavenging of chemisorbed oxygen by H_2O as H_2O concentration increases with increasing conversion, which prevents step 1 and subsequent O_s* reactions (step 16) from reaching equilibrium, because of their kinetic coupling with the CH_4 and H_2O activation steps that remove O_s* (steps 2 and 16, respectively). We note that O_2 chemisorption (eq 1) and the O_s* species formed are required for the ultimate activation of CH_4 (step 2), C_2 products, and H_2O (step 16), irrespective of whether C−H bond activation occurs directly by O_s* species or by the OH radicals derived from such species. Figure 8b shows that differential CH_4 conversion rates become proportional to O_2 pressure at low O_2 concentrations (<0.6 kPa) and modest H_2O pressures (>0.5 kPa), suggesting that O_2 chemisorption steps indeed become kinetically relevant and nearly irreversible (step 20, forward reaction of step 1)

$$O_2 + 2* \xrightarrow{k_{O_2}} 2O_s* \tag{20}$$

$$r = k_{O_2}P_{O_2} \tag{21}$$

where K_{O_2} is approximately 3.6 μmol g^{-1} s^{-1} kPa^{-1}. The rate constant calculated from the collision frequency of O_2 with surfaces at 1073 K is 3×10^7 μmol g^{-1} s^{-1} kPa^{-1}, indicating that sticking coefficients are $\sim 10^{-7}$, a small value consistent with the low concentration of O_s* prevalent during steady-state OCM reactions. We note that, when H_2O is present at significant concentrations, its activation (step 16) is considered to remain much faster in both forward and reverse directions than H-abstraction from CH_4 on the catalyst surface (step 2) at OCM practical conditions where H_2O prevails: therefore, even at low O_2 concentrations, the presence of H_2O (e.g., at high CH_4 conversions) leads to predominant activation of CH_4 via OH-mediated instead of surface (O_s*)-mediated routes.

When prevalent O_2 pressures ensure quasi-equilibrated OH$^\bullet$ concentrations, $CH_4/O_2/H_2O$ and $CH_4/O_2/D_2O$ mixtures should react at similar rates because of the weak nature of the consequent thermodynamic H/D isotope effects on OH/OD concentrations. The data in Table 1 show that the measured KIE for $CH_4/O_2/D_2O$ mixtures, given by

$$\mathrm{KIE} = \left(\frac{k''_{CH_4-OH^\bullet}}{k''_{CH_4-OD^\bullet}}\right)\left(\frac{K_{OH}}{K_{-OD^\bullet}}\right)^{1/4} \tag{22}$$

is 1.08. In eq 22, $K_{OD^\bullet}$ and $k''_{CH_4-OD^\bullet}$ are the equilibrium and rate constants for steps 23 and 24, respectively.

$$O_2 + 2D_2O \overset{K_{OD^\bullet}}{\rightleftharpoons} 4OD^\bullet \tag{23}$$

$$CH_4 + OD^\bullet \xrightarrow{k''_{CH_4-OD^\bullet}} CH_3^\bullet + HDO \tag{24}$$

Using available thermodynamic data for entropy and enthalpy and their temperature dependence,[35] $(K_{OH^\bullet}/K_{OD^\bullet})^{1/4}$ was estimated to be 1.04 at 1073 K. Experimental data for the rate constant of step 24 are unavailable at relevant temperatures (~1000 K), but the $(k''_{CH_4-OH^\bullet}/k''_{CH_4-OD^\bullet})$ ratio is expected to be near unity at 1073 K because both numerator and denominator terms involve the activation of a C−H bond and the formation of a O−H bond.[36,37] Thus, the overall KIE value (eq 22) is expected to be very close to unity, consistent with measured values (1.08, Table 1).

OH-mediated pathways for activation of C−H bonds in CH_4 in kinetically-relevant steps (step 18) would give normal KIE values for $CD_4-O_2-H_2O$ reactants. Table 1 shows that the measured KIE value was 1.44 for these reactants, consistent with kinetically-relevant C−H bond cleavage in CH_4 (step 18). The absence of CH_xD_{4-x} $(0 < x < 4)$ isotopomers during reactions of $CH_4/D_2O/O_2$ or $CD_4/H_2O/O_2$ mixtures confirms the irreversible nature of CH_4 activation steps (steps 2 and 18) and avoids the isotopic dilution of methane that would otherwise prevail. These measured KIE values reflect the combined contributions of surface-catalyzed and OH-mediated C−H bond activation. The rates and corresponding KIE for OH-mediated pathways (the second term in eq 19) can be obtained by subtracting the rates for anhydrous pathways (the first term in eq 19) obtained in section 3.2 from the measured rates for each methane isotopomer. The KIE value for OH-mediated pathways, given by

$$\mathrm{KIE} = \frac{k''_{CH_4-OH^\bullet}}{k''_{CD_4-OH^\bullet}} \tag{25}$$

$$CD_4 + OH^\bullet \xrightarrow{k''_{CD_4-OH^\bullet}} CD_3^\bullet + HDO \tag{26}$$

where $k''_{CH_4-OH^\bullet}$ and $k''_{CD_4-OH^\bullet}$ are rate constants for steps 18 and 26, respectively, is 1.58. We note that this small KIE value for H-abstraction by OH$^\bullet$ is consistent with high reactivity of OH$^\bullet$ leading to relatively product character and to a relatively late transition state, in which C−H bonds would be essentially cleaved. The involvement of less reactive radicals, such as H, O, and HO_2 in C−H bond activation, as discussed in the next section, would lead to KIE values larger than for abstraction of H atoms exclusively by OH.

We examine next the temperature dependence of OH-mediated pathways (the second term in eq 19) by measuring k' at 993−1123 K and O_2 pressures sufficient for quasi-equilibrated O_2 chemisorption (>1.5 kPa) (Figure 3). This activation energy (E''_{app}; 161 ± 9 kJ mol^{-1}) reflects the combined contributions from the activation barrier for H-abstraction from CH_4 by OH$^\bullet$ ($E_{a,OH}$) (eq 18), and the enthalpy for quasi-equilibrated OH radical formation reactions (ΔH_{OH}, step 17)

$$E''_{a,app} = E_{a,OH} + \frac{1}{4}\Delta H_{OH} \tag{27}$$

The reported value of ΔH_{OH} (for step 17) at 1073 K is 650 kJ mol^{-1};[35] thus, eq 27 gives a $E_{a,OH}$ value for C−H bond activation by OH radicals of nearly zero (0 ± 9 kJ mol^{-1}). Such

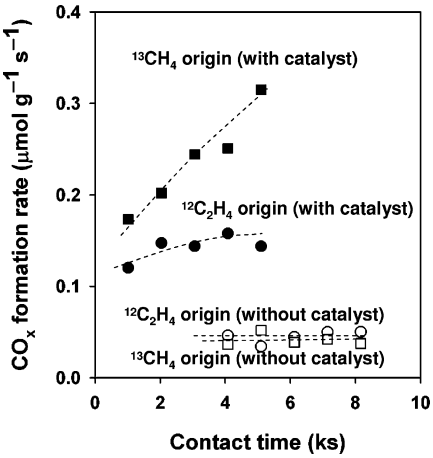

Figure 9. CH_4 conversion and C_2H_4 conversion to CO_x in the presence and the absence of the catalyst, as a function of contact time for $^{13}CH_4/^{12}C_2H_4/O_2$ reaction. Line denotes regressed rates (0.02 g, 1073 K, volume: 475 cm^3, 10.7 kPa $^{13}CH_4$, $CH_4/O_2 = 6$, 0.4 kPa $^{12}C_2H_4$, total pressure 101 kPa, balance He, (●) $^{12}C_2H_4$ conversion to CO_x in the presence of catalyst; (○) $^{12}C_2H_4$ conversion to CO_x in the absence of catalyst; (■) $^{13}CH_4$ conversion to CO_x in the presence of catalyst; (□) $^{13}CH_4$ conversion to CO_x in the absence of catalyst).

small activation barriers (27 kJ mol^{-1})[38] have been previously reported for this reaction (step 18). These activation energies are much smaller than those for surface-mediated C−H bond activation pathways (290 kJ mol^{-1}), confirming the very reactive nature of OH radicals compared with chemisorbed oxygen (O_s*) species and the proposed late nature of transition states for OH-mediated C−H bond activation pathways.

3.5. Effects of H_2O on Primary and Secondary Reactions in Oxidative Coupling of Methane. ***3.5.1. Isotopic Tracer Studies for OCM Reaction Pathways.*** Accurate measurements of kinetic constants in sequential reaction pathways (scheme 1) require the use of isotopic tracers, in which $^{13}CH_4/O_2$ reactants are used together with unlabeled versions of the various $^{12}C_{2+}$ products with and without the presence of H_2O. First, we examine the extent to which purely homogeneous pathways contribute to reactions of CH_4 and OCM products at 1073 K within an empty reactor.

Figure 9 shows rates of $^{13}CH_4$ and $^{12}C_2H_4$ conversion rates to CO_x during reactions of $^{13}CH_4/^{12}C_2H_4/O_2$ mixtures as a function of contact time in an empty reactor and compares these data with those measured in this reactor with $Mn/Na_2WO_4/SiO_2$ (0.02 g). $^{13}CH_4$ and $^{12}C_2H_4$ conversion rates to CO_x were smaller by factors of ~10 and ~4, respectively, when the catalyst was absent. Similar experiments with $^{13}CH_4/^{12}C_2H_6/O_2$ reactants showed that $^{12}C_2H_6$ conversion rates were also ~10 times smaller for purely homogeneous pathways. These data show that kinetically-relevant C−H bond activation in CH_4, C_2H_6, and C_2H_4 molecules occurs predominantly via catalytic routes (both surface-mediated and homogeneous OH-mediated pathways, in which OH radicals form on surfaces).

Reactions of $^{13}CH_4/^{12}C_2H_6/O_2$ and $^{13}CH_4/^{12}C_2H_4/O_2$ mixtures in an empty reactor gave primary $^{13}C_2H_6$ selectivities (from $^{13}CH_4$) much lower (~65%) than when a catalyst was present (~80%) (Figure S3; Supporting Information); these trends reflect the slower formation of CH_3 radicals (from $^{13}CH_4$) when catalytic surfaces are not present. Homogeneous pathways also led to a stronger decrease in C_2 selectivity with increasing contact time than catalytic pathways (Figure S3; Supporting Information), consistent with the prevalence of C−H bond activation by less reactive H-abstractors (such as H and CH_3); these less reactive abstractors more strongly favor activation of molecules, such as C_2H_6, with weaker C−H bonds than those in CH_4 compared with more reactive abstractors. $^{13}CH_4$ conversion rates and $^{13}C_2H_6/^{13}CO_x$ product ratios were not affected by adding $^{12}C_2H_6$ or $^{12}C_2H_4$ to $^{13}CH_4/O_2$ reactants in either empty reactors or in those containing catalysts. These data confirm our previous conclusions that C_2 products cannot give rise to the changes in rates and selectivities observed as conversion increases with increasing contact time (Figure 1a).

TABLE 2: First Order Rate Constants (μmol g^{-1} s^{-1} kPa^{-1}) Measured by Isotopic Tracer Experiments in a Recirculating Reactor for Steps in Scheme *1*, for Surface-Mediated (O_s*) and OH•-Mediated Pathways (0.02 g, 1073 K, Unit Volume: 475−550 cm^3, 10.7 kPa CH_4, $CH_4/O_2 = 6$, 101 kPa Total Pressure, Balance He)

	k_1'	k_2'	k_3'[a]	k_4'[a]	k_5'[b]	k_6'[b]	k_7'[c]	k_8'[d]
surface-mediated	0.05	0.01	1.7	0.14	0.12	0.22	0.59	0.42
OH-mediated[e]	0.16	0.02	1.1	0.12	0.03	0.10	0.36	0

[a] 0.4 kPa $^{12}C_2H_6$ added to $^{13}CH_4-O_2$ mixture. [b] 0.4 kPa $^{12}C_2H_4$ added to $^{13}CH_4-O_2$ mixture. [c] 0.2 kPa $^{12}C_3H_6$ added to $^{13}CH_4-O_2$ mixture. [d] 0.2 or 0.5 kPa ^{13}CO added to $^{12}CH_4-O_2$ mixture. [e] 0.4 kPa H_2O added, from rate differences with and without H_2O.

First-order rate constants for all reactions in Scheme 1 were measured by isotopic tracing using $^{13}CH_4/O_2$ reactants mixed with $^{12}C_2H_6$, $^{12}C_2H_4$, or $^{12}C_3H_6$ in the presence and absence of added H_2O on $Mn/Na_2WO_4/SiO_2$ at 1073 K. Measured rates were extrapolated to zero conversions so that they reflect the H_2O pressure in the starting reactant mixture in both cases (0 or 0.4 kPa H_2O) before H_2O forms via OCM reactions. Table 2 shows rate constants under anhydrous conditions ("surface-mediated" pathways) and via OH-mediated pathways, estimated by comparing data with and without added H_2O. The rate constants for steps 1−7 in Scheme 1 ($k_1'-k_7'$) are all nonzero for OH-mediated pathways, indicating that H_2O provides independent pathways for the activation of C−H bonds in all hydrocarbons. Thus, the beneficial effects of H_2O and the concomitant contributions of OH-mediated pathways must reflect the different (and more desirable) preference with which these pathways activate C−H bonds in CH_4, C_2H_6, C_2H_4, and C_3H_6 relative to the corresponding steps mediated by O_s* species at surfaces, which prevail under anhydrous conditions.

The k_1'/k_2' ratios (k_j for steps in Scheme 1) were larger for OH-mediated (~8) than for surface-mediated (~5) routes (Table 2), consistent with the higher initial C_2 selectivities measured when H_2O was present (Figure 1b). These data reflect an increase in $CH_3^\bullet$ formation rates as a result of additional CH_4 activation pathways mediated by OH radicals and introduced by H_2O molecules and their activation on catalyst surfaces (step 18). These higher radical concentrations increase the rate of bimolecular $CH_3^\bullet$ recombination steps (eq 10) relative to that for unimolecular $CH_3^\bullet$ oxidation to CO_x (eqs 11 and 12). CH_3 radical formation via OH-mediated pathways ($r_{CH_4} = k^* P_{CH_4} P_{O_2}^{1/4} P_{H_2O}^{1/2}$) gives a selectivity ratio of the form

$$\frac{r_{C2}}{r_{CO} + r_{CO_2}} = \frac{1}{2}\left(\sqrt{1 + \frac{4k_{C_2}k'' P_{CH_4} P_{H_2O}^{1/2}}{(k_{CO} + k_{CO_2} P_{O_2}^{1/2})^2 P_{O_2}^{3/4}}} - 1\right) \quad (28)$$

which simplifies to eq 29 at the high prevalent selectivity ratios (>4)

$$\frac{r_{C2}}{r_{CO} + r_{CO_2}} = \sqrt{\frac{k_{C_2} k'' P_{CH_4} P_{H_2O}^{1/2}}{(k_{CO} P_{O_2}^{1/2} + k_{CO_2})^2 P_{O_2}^{3/4}}} \quad (29)$$

The ratio expected from rate constants measured under anhydrous conditions is ~13, while measured values are ~8, apparently because of small contributions from less reactive (and more sensitive to C−H bond strengths) radicals (e.g., H, HO_2), which would give ratios higher than predicted from eq 29, because of higher k_{CO} and k_{CO_2} values.

Next, we compare the relative rates of activation of C−H bonds in CH_4, C_2H_6, and C_2H_4 via H-abstraction on surfaces (O_s*) and with OH radicals in the context of the rate constants reported in Table 2. The ubiquitous decrease in C_{2+} selectivities observed with increasing CH_4 conversion and contact time reflects the relative reactivities of reactants and products, which arises, in turn, from their different rate constants. Figure 10 shows the ratios of C_2H_6 and C_2H_4 activation rate constants relative to those for CH_4 activation via surface-catalyzed and OH-mediated routes together with the homolytic dissociation energies for each of the C−H bonds involved. These ratios are smaller for OH-mediated than for surface-mediated pathways, consistent with the higher C_2 yields attained when H_2O was present (Figure 1b). These rate constant ratios decreased monotonically with increasing C−H bond energies for OH-mediated pathways (Figure 10), consistent with the sole kinetic-relevance and homolytic character of the H-abstraction steps involved. Rate constant ratios agree well with those expected from ratios reported for the corresponding rate constants for H-abstraction by OH radicals via homogeneous reactions at 1073 K (CH_4, 1.6×10^{12}; C_2H_6, 5.5×10^{12}; C_2H_4, 1.2×10^{12} cm^3 mol^{-1} s^{-1}),[38] consistent with the involvement of these gas-phase radicals in the kinetically-relevant steps for the activation of C−H bonds in CH_4 and C_2 hydrocarbons. The activation barriers for such steps follow Brønsted−Evans−Polanyi relations[39]

$$|\Delta E_a| = \alpha \Delta |\Delta H_r^\circ|$$

where α is the Brønsted−Evans−Polanyi parameter, ΔE_a is the difference between the activation energies for two homologous steps, and $\Delta|\Delta H_r|$ is the difference between the respective reaction enthalpies (in this case given by differences in C−H bond strengths). Similar monotonic trends were not evident for surface-mediated pathways (Figure 10), for which C_2H_4 molecules appear to react much faster than expected from the strength of their C−H bonds, apparently because their π-electrons lead to stronger interactions with Lewis acid sites on oxide catalyst surfaces.

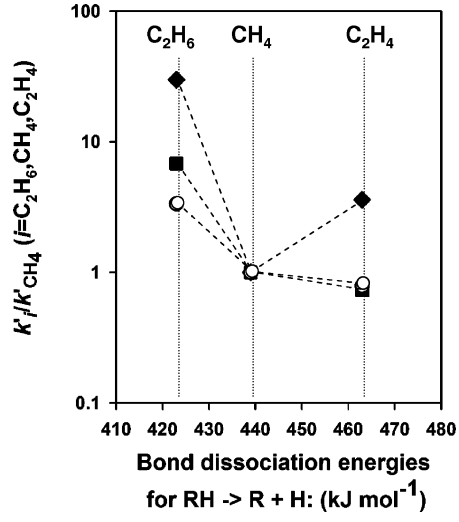

Figure 10. Ratio of rate constants for conversion of C_2H_6 ($k'_3 + k'_4$) and C_2H_4 ($k'_5 + k'_6$) to that for conversion of CH_4 ($k'_1 + k'_2$) as a function of C−H bond dissociation energies. (◆) Surface-mediated pathway; (■) OH-mediated pathway; (○) H abstraction by OH radicals in the gas-phase.[38]

The combined rate constants for C_2H_6 activation ($k'_3 + k'_4$) were ~30 times larger than for CH_4 activation ($k'_1 + k'_2$) in the case of the surface-mediated pathways prevalent under anhydrous conditions, as expected from the weaker C−H bonds in C_2H_6 (423 kJ mol^{-1}) compared with those in CH_4 (439 kJ mol^{-1}).[32] This ratio was much smaller (6.8) for OH-mediated pathways, even though both surface-mediated and OH-mediated routes involve kinetically-relevant C−H bond activation in CH_4 and C_2H_6. Thus, the different specificity for C−H bond activation via these pathways must reflect differences in the reactivity of the two abstractors involved (i.e., $OH^\bullet$ and O_s*) and in their sensitivity to C−H bond energies.

Abstractors that form stronger bonds with H-atoms react with lower sensitivity to the strength of the C−H bond being activated. We have previously shown that reactions with energetic H-abstractors, such as OH radicals, react less selectively with the weaker C−H bonds in HCHO (relative to stronger C−H bonds in CH_4) than more stable radicals, such as O and HO_2.[40] OH radicals are among the most thermodynamically unstable and reactive H-abstractors; they form very strong O−H bonds within the stable H_2O molecules formed in such processes.[18] The ratio of the rate constants for H-abstraction from ethane and methane by gas-phase OH radicals ($k^{OH}_{C_2H_6}/k^{OH}_{CH_4}$) is 3.3−4.4.[14,38] OH-mediated pathways in OCM reactions give values slightly higher than these (6.8; Table 2), but much smaller than for surface-mediated pathways (30). We surmise that measured $k^{OH}_{C_2H_6}/k^{OH}_{CH_4}$ ratios are higher than reported for H-abstraction by OH radicals,[14,38] because of parallel contributions from $CH_3^\bullet + C_2H_6 \rightarrow CH_4 + C_2H_5^\bullet$ reactions and perhaps also from reactions with O and HO_2 radicals, which are less reactive than OH radicals. Contributions from these less reactive radicals to C−H bond activation would lead to KIE values larger than from exclusive OH-mediated H-abstraction from CH_4 (Table 1), as mentioned in section 3.4.

C_2H_4 conversion rate constants ($k'_5 + k'_6$) were ~5 times larger than for CH_4 conversion ($k'_1 + k'_2$) for surface-mediated pathways prevalent under anhydrous conditions, even though C−H bonds in C_2H_4 are significantly stronger than in CH_4 reactants. This high C_2H_4 reactivity appears to reflect the specific and preferential binding of C_2H_4 on oxide surfaces,[41] compared with CH_4 and C_2H_6.[30] In contrast, C_2H_4 was found to be less reactive than CH_4 via OH-mediated pathways ($(k'_5 + k'_6)/(k'_1 + k'_2) \sim 0.7$; Table 2). This reflects the homolytic C−H bond activation routes involved in OH-mediated pathways, which rigorously reflect the relative energies of the C−H bonds involved in the activation of CH_4 and C_2H_4. The reported rate of homogeneous H-abstraction from C_2H_4 by OH radicals is also smaller than for CH_4,[38] and the ratio of C_2H_4 to CH_4 conversion rates reported here (0.7 at 1073 K) is very similar to that reported for gas-phase radical reactions ($k^{OH}_{C_2H_4}/k^{OH}_{CH_4} = 0.8$).[14,38] These low $k_{C_2H_4}/k_{CH_4}$ ratios reflect the stronger C−H bonds in C_2H_4 compared with CH_4, as well as the introduction of homogeneous pathways that do not involve surface sites and the concomitant preferential binding of C_2H_4. Surface-mediated pathways that prevail under anhydrous conditions account for the high reactivity of C_2H_4 during OCM reactions and for the preferential removal of these valuable products as CH_4 conversion increases.

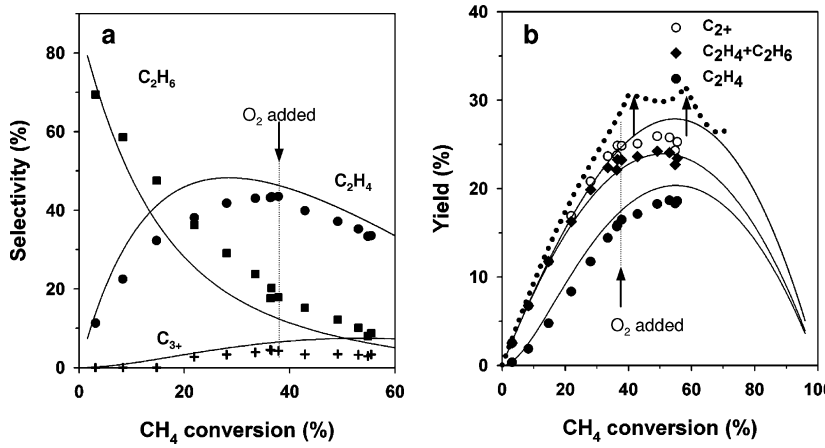

Figure 11. Product selectivities (a) and yields (b) as a function of CH_4 conversion measured in a recirculating batch reactor. The solid curves denote model prediction with Scheme 1 and rate constants in Table 2 and the dotted curve denotes the ChemKin model including quasi-equilibrated OH radical formation (0.02 g, 1073 K, volume: 550 cm^3, 4.0 kPa CH_4, 1.3 kPa O_2 (initial), 1.5 kPa O_2 (added), total pressure 101 kPa, balance He, ChemKin model: 1073 K, 10 kPa CH_4, 1.7 kPa O_2, total pressure 101 kPa).

Small concentrations of higher hydrocarbons (predominantly C_3H_6) were detected as CH_4 conversion increased, because recombination reactions of methyl radicals with C_2 products and respective radicals become important as C_2 concentrations increase (e.g., $C_2H_3^\bullet + CH_3^\bullet \rightarrow C_3H_6$; $C_2H_4 + CH_3^\bullet \rightarrow C_3H_7^\bullet \rightarrow C_3H_6 + H^\bullet$). Therefore, we include C_3H_6 reactions in Scheme 1. The rate of C_3 formation and oxidation were probed by isotopic tracing using $^{13}CH_4/^{12}C_3H_6/O_2(/H_2O)$ reactants. The k_7'/k_1' ratios for OH-mediated pathways (~2) of C_3H_6 are much smaller than for surface-mediated pathways (~12) (Table 2). The rate constants for C_3H_6 oxidation (k_7') are much larger than for C_2H_6 (k_4') or C_2H_4 (k_6') oxidation via the respective OH-mediated and surface-catalyzed pathways, consistent with the weak nature of allylic C−H bonds in C_3H_6 (372 kJ mol^{-1}).[32] These results suggest that chain growth contributes significantly to yield losses in OCM reactions, as proposed previously.[13] The observed selectivity to higher hydrocarbons (C_{3+}) was relatively low (~4.5%) at the modest pressures used here (4−10 kPa CH_4). Higher pressures, required for relevant OCM practice, favor radical recombination and may lead to higher C_{3+} formation rates and to more significant C_{2+} yield losses via rapid oxidation of higher alkanes and alkenes.

Figure 11, panels a and b, shows measured OCM product selectivities and yields, together with predictions from a kinetic treatment based on the steps in Scheme 1 and independently measured rate constants for surface-catalyzed and OH-mediated routes (Table 2). Maximum C_2 and C_{2+} yields were 24% and 26% (Figure 11b), respectively, similar to the highest reported yields.[8] The network in Scheme 1 accurately describes measured yields as a function of CH_4 conversion (Figure 11b). In contrast, rate constants for surface-mediated pathways predict maximum C_{2+} yield of only 14%,[18] because of the high k_6'/k_1' (~4) and k_7'/k_1' (~12) ratios for the surface-mediated pathways that prevail under anhydrous conditions. Maximum attainable C_{2+} yields are limited in practice by the relative reactivity of C_2 (and C_{3+}) and CH_4 at conditions where highly reactive OH radicals predominantly account for the kinetically-relevant H-abstraction from hydrocarbon reactants and products.

3.5.2. Simulation of OH-Mediated Pathway Model and Attainable OCM Yields. Next, we report simulation results to illustrate the effects of OH radical formation on OCM rates and selectivities, using available ChemKin codes[26] and reported rate and equilibrium constants for relevant gas phase reactions.[14] Previous studies[13,24,42,43] have treated the coupling of homogeneous and surface-catalyzed routes via the formation of organic radicals through C−H bond activation on O_s* species. Here, we include a fast surface reaction that forms equilibrium concentrations of OH radicals, which are not attainable via purely homogeneous kinetic routes

$$O_2 + 2H_2O \rightleftarrows 4OH^\bullet$$

This is implemented by using arbitrarily large pre-exponential factors for the forward and reverse steps of this reaction, while maintaining their rate ratio consistent with the thermodynamics of the overall reaction. Figure 11b shows C_{2+} yields predicted by these simulations. At conditions similar to those used in our experiments (10 kPa CH_4, O_2 1.7 kPa, 1073 K) and with O_2 addition after its depletion (the arrows in Figure 11b), C_{2+} yields are similar to measured values (~30%, Figure 11b). This agreement with experiment is reassuring in view of the absence of undesired side reactions of C_{2+} products on catalyst surfaces in this model and suggests that OH radicals indeed account for most H-abstraction events at relevant H_2O concentrations.

These simulations were extended to reactant pressures and temperatures unattainable in our experimental setup within safe operating regimes but potentially useful in OCM industrial practice. Throughout these simulations, we have maintained quasi-equilibrated OH radical formation steps; therefore, C_2 yields represent upper bounds, because they neglect less selective surface-mediated steps or OH concentrations below equilibrium levels. The inlet ratio of CH_4 to O_2 was set to 6, as in our experiments, and O_2 was added after its pressure decreased below 0.1 kPa until C_2 yields reached a maximum value. Figure 12 shows the highest attained C_2 yields at each temperature and CH_4 inlet pressure. Higher CH_4 pressures decreased C_2 yields because they favor chain growth and the formation of reactive C_{3+} species, which form CO_x more rapidly than CH_4 or C_2H_6. Temperatures above 1073 K increased C_2 yields, because the activation barrier for OH reactions with CH_4 is higher than for the respective reaction with C_2H_6, C_2H_4, and C_{3+} hydrocarbons.[14] These simulations show, however, an optimum intermediate temperature for maximum C_2 yields (e.g., ~1250 K at 10 kPa CH_4) partly because, for a given conversion, the ratio of the concentrations of C_2H_3 to CH_3 increases with temperature so that higher hydrocarbon formation (C_3, C_4; e.g., $CH_3 + C_2H_3 \rightarrow C_3H_6$) (and their subsequent combustion) becomes comparatively faster than C_2 formation ($CH_3 + CH_3 \rightarrow C_2H_6$) in this kinetic model. In practice, the higher measured activation energies for surface-mediated pathways (290 kJ

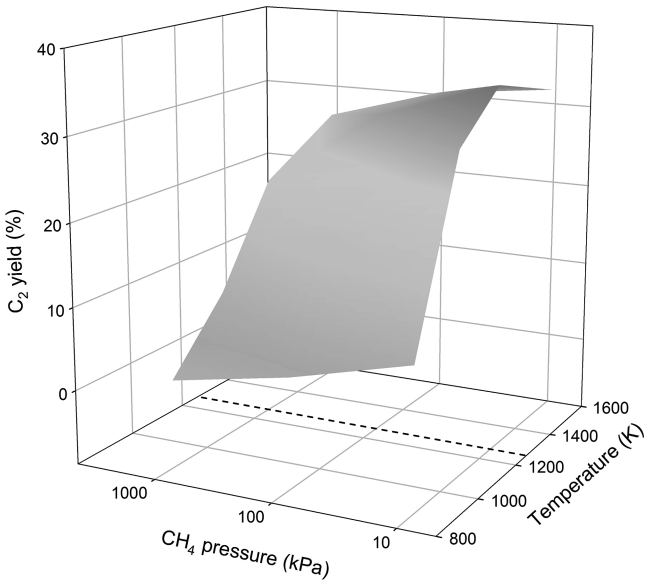

Figure 12. Maximum C_2 yield calculated by ChemKin simulation, as a function of CH_4 pressure and reaction temperature using a reported kinetic database.[14] Dashed line indicates the temperature giving the highest C_2 yield ($CH_4/O_2 = 6$. O_2 addition after its reduction to <0.1 kPa to reach the maximum C_2 yield).

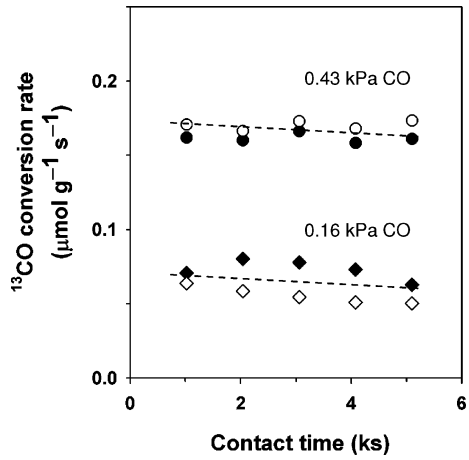

Figure 13. ^{13}CO conversion rate as a function of contact time during the reaction of $^{12}CH_4/^{13}CO/O_2(/H_2O)$ mixture measured in a recirculating reactor (0.02 g, 1073 K, volume: 550 cm^3, 10.7 kPa $^{12}CH_4$, 1.8 kPa O_2, total pressure 101 kPa, balance He, (●) 0.43 kPa ^{13}CO; (○) 0.43 kPa ^{13}CO, 0.4 kPa H_2O; (◆): 0.16 kPa ^{13}CO; (◇) 0.16 kPa ^{13}CO, 0.4 kPa H_2O).

mol^{-1}) compared with OH-mediated pathways (161 kJ mol^{-1}; Figure 3) would lead to increasing contributions from less selective surface-mediated routes as the reaction temperature increases, making these higher C_2 yields at high temperature unattainable.

We have also examined pathways for CO oxidation during OCM using $^{12}CH_4/^{13}CO/O_2$ isotopic mixtures (Figure 13) with and without added H_2O; H_2O can introduce water−gas shift pathways ($CO + H_2O \rightleftarrows CO_2 + H_2$) that form CO_2 without direct involvement of O_2. Measured ^{13}CO oxidation rates were proportional to ^{13}CO pressure and independent of H_2O concentrations. These results indicate that CO oxidation occurs via surface-mediated pathways on O_s* species that also activate C−H bonds and that water-gas shift reactions do not occur at detectable rates on $Mn/Na_2WO_4/SiO_2$ even at >1000 K. First-order CO oxidation rate constants (Scheme 1) are significantly larger than for CH_4 activation with O_s* ($k_8'/(k_1' + k_2') \sim 7$, Table 2), suggesting that CO_2 is formed preferentially instead of CO via surface-mediated pathways. The presence of H_2O increased both ^{12}CO and $^{12}CO_2$ formation rates (from $^{12}CH_4$) because OH-mediated CH_4 activation routes also form ^{12}CO and $^{12}CO_2$ (k_2'; Scheme 1). These results also show that OH radicals do not react with CO to form CO_2 either directly (to form CO_2 and H) or via reactions with other species derived from OH radicals.

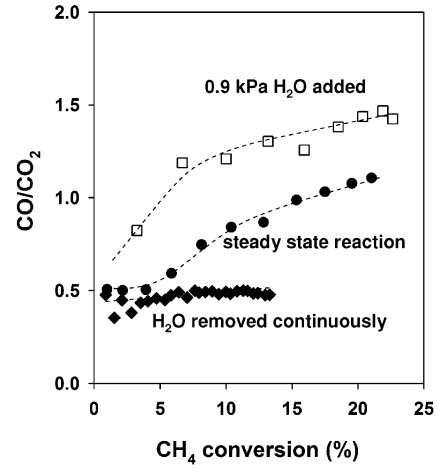

Figure 14. CO/CO_2 ratio as a function of CH_4 conversion measured in a recirculating batch reactor (0.02 g, 1073 K, volume: 275−650 cm^3, 10.7 kPa CH_4, 1.8 kPa O_2, 101 kPa total pressure, balance He, (◆): H_2O removed continuously; (●): steady state reaction (H_2O concentration increases during reaction); (□): 0.9 kPa H_2O added).

Figure 14 shows measured CO/CO_2 ratios for experiments in which water was (i) added; (ii) allowed to accumulate during OCM; or (iii) removed as it formed in OCM reactions. CO/CO_2 ratios remained relatively low (~0.5), even at high CH_4 conversions, when H_2O was continuously removed because prevalent surface-mediated pathways convert hydrocarbons predominantly to CO_2 (step 9). As H_2O formed in OCM reactions were allowed to accumulate, CO/CO_2 ratios increased with increasing conversion and H_2O concentration. The addition of H_2O to CH_4-O_2 reactants gave higher CO/CO_2 ratios, because OH-mediated pathways lead to radical species that preferentially form CO from hydrocarbons via homogeneous pathways. CH_4 and C_2 oxidation in empty reactors led to very high CO/CO_2 ratios (>5), consistent with the preferential formation and significant stability of CO in homogeneous oxidation pathways and with the known free radical pathways that form significant amounts of CO during homogeneous combustion at low temperatures.[38]

3.6. Effects of O_2 Concentrations on Maximum Attainable C_2 Yields in OCM Reactions. Low O_2 pressures can improve C_2 yields when CH_4 activation steps that form C_2 molecules (r_1; Scheme 1) depend less sensitively on O_2 pressures than the steps leading to the combustion of CH_4 (r_2) or C_{2+} products (r_4, r_6, r_7).[14] Figure 1, panels a and b, shows differential CH_4 conversion rates and (integral) C_{2+} selectivities, respectively, at two O_2 pressures (open circles for 0.9 kPa O_2; others for 1.8 kPa O_2). CH_4 conversion rates increased with O_2 pressure, consistent with the rates predicted by eq 19. Low O_2 pressures led to higher C_2 selectivities at CH_4 conversions below <10%, but C_2 selectivities at higher conversions became almost insensitive to O_2 pressure. Thus, low O_2 pressures seem to favor high initial C_2 selectivities (i.e., r_1/r_2 in Scheme 1) but do not lead to higher selectivities or yields at relevant levels of CH_4 conversion.

The effects of O_2 concentrations on attainable C_2 yields at higher CH_4 conversions (>15%) were probed in a gradientless

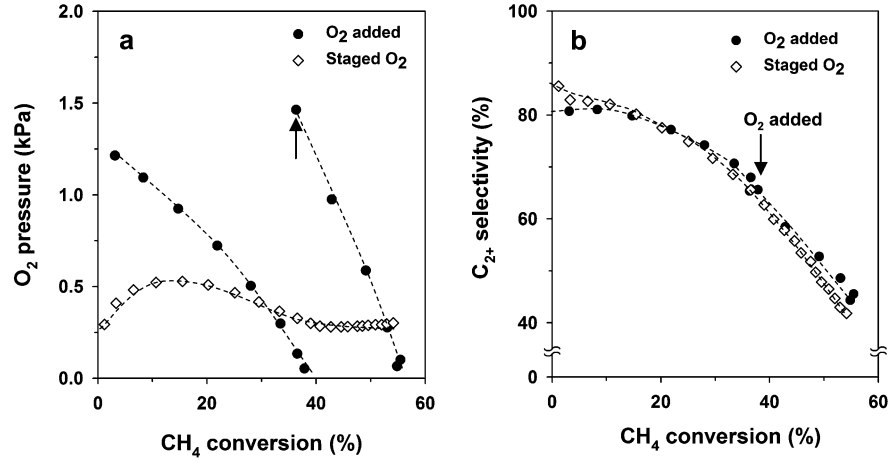

Figure 15. Effects of O_2 partial pressure (a) on C_{2+} selectivity (b) as a function of CH_4 conversion measured in a recirculating batch reactor (0.02 g, 1073 K, volume: 550 cm^3, 4.0 kPa CH_4, 101 kPa total pressure, balance He, (●) O_2 added; (◇) staged O_2 introduction).

TABLE 3: Rate of CH_4 Conversion and Rate Ratio of CH_4 Conversion for C_2 Formation to CO_x Formation at Different Kinetic Regimes (r_1, r_2 in Scheme 1, See Eqs 15, 29, and 31)

	surface O*	gas phase OH	O_2 chemisorption limiting
r_{CH_4}	$k'(CH_4)^1(O_2)^{0.5}$	$k''(CH_4)^1(O_2)^{0.25}(H_2O)^{0.5}$	$k_{O_2}(O_2)$
r_1/r_2	$[(k'k_{C_2}P_{CH_4})/((k_{CO}P_{O_2}^{1/2} + k_{CO_2})^2P_{O_2}^{1/2})]^{1/2}$	$[(k_{C_2}k''P_{CH_4}P_{H_2O}^{1/2})/((k_{CO}P_{O_2}^{1/2} + k_{CO_2})^2P_{O_2}^{3/4})]^{1/2}$	$(k_{C_2}k_{O_2})^{1/2}/(k_{CO}P_{O_2}^{1/2} + k_{CO_2})$

recirculating reactor by introducing additional oxygen, either after it was depleted or continuously as it was consumed (staged oxygen introduction).[14,24] The latter strategy would rigorously mimic the continuous introduction of O_2 along a tubular reactor via selectively permeable walls or distributed injectors, which have been proposed as effective strategies to improve C_2 yields in OCM reactors.[24] Figure 15b compares C_{2+} selectivities as a function of CH_4 conversion for the O_2 pressure temporal profiles in Figure 15a. C_2 selectivities at CH_4 conversions below 10% were indeed improved by staging O_2 co-reactants, but such improvements became much smaller and nearly imperceptible as CH_4 conversion levels increased to those required for even modest C_2 yields (Figure 15b). We conclude that O_2 staging strategies do not lead to practical gains in C_2 yields because C−H bond activation in CH_4 and C_{3+} hydrocarbons depend similarly on O_2 pressure, whether activation occurs via surface-mediated or OH-mediated routes.

Next, we discuss the effects of O_2 pressure on primary selectivities (r_1/r_2) for the three relevant kinetic regimes (i) surface-mediated pathways (the first term in eq 19); (ii) OH-mediated pathways (the second term in eq 19); and (iii) pathways limited by O_2 chemisorption (eq 21). When O_2 chemisorption becomes irreversible (step 20), eqs 10−12 and 21 lead to primary C_2 selectivities given by

$$\frac{r_{C2}}{r_{CO} + r_{CO_2}} = \frac{1}{2}\left(\sqrt{1 + \frac{4k_{C_2}k_{O_2}}{(k_{CO}P_{O_2}^{1/2} + k_{CO_2})^2}} - 1\right) \tag{30}$$

which becomes, at high values of these selectivity ratios (>4):

$$\frac{r_{C2}}{r_{CO} + r_{CO_2}} = \frac{\sqrt{k_{C_2}k_{O_2}}}{(k_{CO}P_{O_2}^{1/2} + k_{CO_2})} \tag{31}$$

The equations for these ratios when OCM reactions occur via the three routes mentioned above are shown in Table 3. The effects of O_2 pressure on selectivity are stronger for OH-mediated pathways (eq 29, $r_1/r_2 \sim (A^2\ P_{O_2}^{3/4})^{-1}$, where $A = k_{CO}P_{O_2}^{1/2} + k_{CO_2}$) than for surface-mediated pathways (eq 15, $r_1/r_2 \sim (A^2\ P_{O_2}^{1/2})^{-1}$). For O_2-limiting pathways, this selectivity ratio becomes proportional to $r_1/r_2 \sim (A)^{-2}$ (eq 31) and least sensitive to O_2 pressure. This accounts, at least in part, for the preferential effects of O_2 pressure on selectivity at low conversions (Figure 1) and for the apparent insensitivity to O_2 pressures at high conversions that lead to irreversible O_2 chemisorption steps and low O_s* coverages. These trends reflect, in turn, the concurrent decrease in O_2 chemisorption rates and the increase in the rate of scavenging of chemisorbed oxygen via OH-mediated CH_4 activation pathways, which become faster as H_2O concentrations increase with increasing conversion levels.

We probe next the sensitivity of each reactant and product conversion rate ($r_1 - r_7$) to O_2 pressure. In the absence of H_2O, surface oxygens (O_s*) are involved in kinetically-relevant C−H bond activation steps for both CH_4 reactants and OCM products and rates are proportional to O_s* concentrations (and thus to $P_{O_2}^{0.5}$) for all C−H bond activation steps. As H_2O forms during OCM reactions, quasi-equilibrated H_2O−O_s* reactions form OH radicals that become the predominant H-abstractors and all C−H bond activation rates become proportional to $P_{O_2}^{0.25}$ (eq 19) when O_2 chemisorption (step 1) is quasi-equilibrated and to $P_{O_2}^{1}$ as this latter step becomes irreversible and kinetically-relevant (Figure 8b, step 20).

The dependence of hydrocarbon conversion rates (CH_4, C_2H_6, C_2H_4, and C_3H_6) on O_2 pressure is the same for all hydrocarbons and a given H-abstractor ($OH^{\bullet}$ or O_s*). The data in Figure 15b show that C_2 yields are essentially unaffected by O_2 pressure. At CH_4 conversions above 40%, C_{2+} selectivities were actually lower for staged O_2 introduction than for co-fed experiments. At the low O_2 pressures prevalent in these staged experiments, the concurrent presence of H_2O leads to irreversible and rate-determining O_2 chemisorption steps at all conversion levels; in this kinetic regime, O_2 pressures do not affect primary C_2 selectivities (r_1/r_2) at low conversions (eq 31, Table 3), as discussed above. Low O_2 pressures, however, decrease the rate of all surface-catalyzed reactions involving O_s*, including those leading to OH radicals involved in homogeneous C−H bond activation steps, because they all have positive kinetic orders

in O_2 (eqs 19 and 21). The consequent decrease in CH_3 concentrations leads to lower C_2 selectivities, because of the bimolecular nature of CH_3 recombination steps that form C_2 (eq 10), which depend on CH_3 concentrations more strongly than the unselective unimolecular pathways that form CO from CH_3 radicals (eqs 11 and 12).

We note that similar experiments and kinetic analyses on SrO_x/La_2O_3 solids, which also catalyze OCM,[44] did not detect significant effects of H_2O on rates or selectivities. These catalysts gave lower maximum yields than $Mn/Na_2WO_4/SiO_2$. These findings indicate that OH formation rates depend sensitively on the identity of the catalyst and that the unique selectivity and yields reported on $Mn/Na_2WO_4/SiO_2$ reflect, at least in part, its ability to form quasi-equilibrated OH radical concentrations from H_2O-O_2 at conditions also required for surface-mediated OCM pathways.

Maximum OCM yields would require conditions in which OH radicals act as the predominant H-abstractors, but which also maintain quasi-equilibrated O_2 chemisorption steps. OH-mediated pathways are more sensitive to O_2 pressure than surface O_s*-mediated pathways; thus, decreasing O_2 pressures would improve selectivities as long as OH concentrations can be maintained at equilibrium levels, a requirement that can be met only at sufficiently high O_2 pressures. These findings and interpretations suggest that intermediate O_2 pressures are optimal and that these optimal values depend sensitively on the prevalent H_2O concentration at a given point in the reactor and on its concomitant effect on the rate OH-mediated pathways. The consequences of these optimization strategies can be accurately probed as a result of the unprecedented detail in the kinetic models that we report here for the first time and of the use of experimental reactors that can be used to rigorously validate the kinetic models and their use in these staging protocols.

4. Conclusions

Attainable C_2 yields for OCM are limited by the intrinsic reactivity of C_2 (and C_{3+}) relative to CH_4 at conditions where highly reactive OH radicals are responsible for the kinetically-relevant H-abstraction from each hydrocarbon. Our rigorous kinetic measurements revealed the supplementary and predominant C−H activation pathways mediated by OH free radicals formed from H_2O/O_2 mixtures during OCM on $Mn/Na_2WO_4/SiO_2$. Isotope effects and scrambling experiments using CD_4/CH_4 and/or D_2O/H_2O showed that C−H bond activation was irreversible and kinetically-relevant both in the presence and the absence of H_2O, and that O−H bond activation steps were not involved in the kinetically-relevant steps. Scrambling experiments using $^{18}O_2-^{16}O_2$ showed that O_2 dissociation was quasi-equilibrated only at high O_2/H_2O ratios. At low O_2/H_2O ratios, O_2 chemisorption steps become no longer quasi-equilibrated and nearly irreversible, and limit the overall conversion rates, where the OCM selectivity is insensitive to O_2 pressures. Isotopic tracer studies using $^{13}CH_4/O_2(/H_2O)$ with $^{12}C_2H_6$, $^{12}C_2H_4$ or $^{12}C_3H_6$ mixtures showed that rate constant ratios $k_{C_2H_6}/k_{CH_4}$ and $k_{C_2H_4}/k_{CH_4}$ were smaller for OH-mediated pathways than for surface mediated pathways, consistent with improved C_2 selectivities and yields in the presence of H_2O, which are ascribed to (1) enhanced steady-state CH_3 radical concentrations introduced by OH-mediated pathways and the second-order nature of CH_3 radicals for their coupling, compared to the first-order nature of their oxidation process, (2) the reactive nature of OH radicals which give unselective H-abstraction to intrinsic C−H bond strengths in hydrocarbons compared to O_s* as less reactive H-abstractors, and (3) avoiding strong adsorption of C_2H_4 on surfaces that favor its oxidation, by the gas-phase OH radical routes. C_3 and higher hydrocarbon formation, which have bimolecular nature of carbonaceous radicals and are favored at high pressures, in turn lead to rapid combustion and reduce maximum attainable yields. Mechanism-based rate equations comprising rate-determining C−H bond activation by surface-mediated and OH-mediated routes accurately describes the effects of pressure and residence time on rates and attainable C_2 yields. The maximum C_2 yields measured were unaffected by staging introduction of O_2 in OCM reactors because of the same dependence of O_2 pressure on the C−H bond activation rates for CH_4, C_2H_6, and C_2H_4 and the insensitivity of OCM selectivity to O_2 pressure at O_2 chemisorption limiting conditions.

Acknowledgment. This study was supported by BP as part of the Methane Conversion Cooperative Research Program at the University of California at Berkeley. The authors acknowledge Drs. Ayman D. Allian, Aditya Bhan, Josef Macht, and Xinyu Xia, and Mr. Rajamani Gounder of the University of California at Berkeley for extensive technical comments and suggestions about the contents and interpretations in this manuscript. The technical guidance of Drs. Theo Fleisch and Sander Gaemers of BP are also acknowledged with thanks.

Supporting Information Available: Additional explanation of experimental results. This material is available free of charge via the Internet at http://pubs.acs.org.

References and Notes

(1) Keller, G. E.; Bhasin, M. M. *J. Catal.* **1982**, *73*, 9.
(2) Lunford, J. H. *Catal. Today* **2000**, *63*, 165.
(3) Lercher, J. A.; Bitter, J. H.; Steghuis, A. G.; van Ommen, J. G.; Seshan, K. In *Environmental Catalysis*; Jannsen, F. J. J. G., van Santen, R. A., Eds.; Imperial College Press: London, 1999; pp 103−126.
(4) Fang, X.; Li, S.; Lin, J.; Gu, J.; Yang, D. *J. Mol. Catal. (China)* **1992**, *6*, 427.
(5) Wang, D.; Rosynek, M. P.; Lunsford, J. H. *J. Catal.* **1995**, *155*, 390.
(6) Pak, S.; Qiu, P.; Lunsford, J. H. *J. Catal.* **1998**, *79*, 222.
(7) Pak, S.; Lunsford, J. H. *Appl. Catal., A* **1998**, *168*, 131.
(8) Palermo, A.; Vazquez, J. P. H.; Lee, A. F.; Tikhov, M. S.; Lambert, R. M. *J. Catal.* **1998**, *177*, 259.
(9) Ito, T.; Wang, J.-X.; Lin, C.-H.; Lunsford, J. H. *J. Am. Chem. Soc.* **1985**, *107*, 5062.
(10) Campbell, K. D.; Lunsford, J. H. *J. Phys. Chem.* **1988**, *92*, 5792.
(11) Morales, E.; Lunsford, J. H. *J. Catal.* **1989**, *118*, 255.
(12) Labinger, J. A. *Catal. Lett.* **1988**, *1*, 371.
(13) Labinger, J. A.; Ott, K. C. *J. Phys. Chem.* **1987**, *91*, 2682.
(14) Mims, C. A.; Mauti, R.; Dean, A. M.; Rose, K. D. *J. Phys. Chem.* **1994**, *98*, 13357.
(15) Reyes, S. C.; Iglesia, E.; Kelkar, C. P. *Chem. Eng. Sci.* **1993**, *48*, 2643.
(16) Reyes, S. C.; Kelkar, C. P.; Iglesia, E. *Catal. Lett.* **1993**, *19*, 167.
(17) Batiot, C.; Hodnett, B. K. *Appl. Catal., A* **1996**, *137*, 179.
(18) Takanabe, K.; Iglesia, E. *Angew. Chem., Int. Ed.* **2008**, *47*, 7689.
(19) Anderson, L. C.; Xu, M.; Mooney, C. E.; Rosynek, M. P.; Lunsford, J. H. *J. Am. Chem. Soc.* **1993**, *115*, 6322.
(20) Hewett, K. B.; Anderson, L. C.; Rosynek, M. P.; Lunsford, J. H. *J. Am. Chem. Soc.* **1996**, *118*, 6992.
(21) Hewett, K. B.; Rosynek, M. P.; Lunsford, J. H. *Catal. Lett.* **1997**, *45*, 125.
(22) Gaffney, A. M. U.S. Patent, 4788372.
(23) Leyshon, D. W. U.S. Patent, 4801762.
(24) Androulakis, I. P.; Reyes, S. C. *AIChE J.* **1999**, *45*, 860.
(25) Coronas, J.; Santamaría, J. *Catal. Today* **1999**, *51*, 377.
(26) ChemKin, Reaction Design CHEMKIN 4.1.
(27) Brunauer, S.; Emmett, P. H.; Teller, E. *J. Am. Chem. Soc.* **1938**, *60*, 309.
(28) Iglesia, E.; Baumgartner, J. E.; Price, G. L.; Rose, K. D.; Robbins, J. L. *J. Catal.* **1990**, *125*, 95.
(29) Roos, J. A.; Korf, S. J.; Veehof, R. H. J.; van Ommen, J. G.; Ross, J. R. H. *Appl. Catal.* **1989**, *52*, 131.
(30) Lacombe, S.; Zanthoff, H.; Mirodatos, C. *J. Catal.* **1995**, *155*, 106.

(31) Otsuka, K.; Said, A. A.; Jinno, K.; Komatsu, T. *Chem. Lett.* **1987**, 77.

(32) Blanksby, S. J.; Ellison, G. B. *Acc. Chem. Res.* **2003**, *36*, 255.

(33) Hutchings, G. J.; Woodhouse, J. R. J. *Chem. Soc. Faraday Trans.* **1 1989**, *85*, 2507.

(34) The rate constant optimization is calculated using Athena Visual Studio Version: 10.7. Stewart and Associates Engineering Software, Inc. More details are available in Supporting Information (Scheme S1, Table S1, and Figure S2).

(35) Chase, M. W., Jr. *J. Phys. Chem. Ref. Data* **1998**, 1 NIST-JANAF Themochemical Tables, Fourth Edition, Monograph 9.

(36) Masgrau, L.; Gonzalez-Lafont, A.; Lluch, J. M. *J. Chem. Phys.* **2001**, *115*, 4515.

(37) Masgrau, L.; Gonzalez-Lafont, A.; Lluch, J. M. *J. Chem. Phys.* **2001**, *114*, 2154.

(38) GRI-Mech v.3.0. Smith, G. P.; Golden, D. M.; Frenklach, M.; Moriarty, N. W.; Eiteneer, B.; Goldenberg, M.; Bowman, C. T.; Hanson, R. K.; Song, S.; Gardiner, W. C., Jr.; Lissianski, V. V.; Qin, Z. http://www.me.berkeley.edu/gri_mech/.

(39) Boudart, M.; Djéga-Mariadassou, G. *Kinetics of Heterogeneous Catalytic Reactions*; Princeton University Press: Princeton, NJ, 1984; p 121.

(40) Zalc, J. M.; Green, W. H.; Iglesia, E. *Ind. Eng. Chem. Res.* **2006**, *45*, 2677.

(41) Dumesic, J. A.; Rudd, D. F.; Aparicio, L. M.; Rekoske, J. E.; Treviño, A. A. *The Microkinetics of Heterogeneous Catalysis*; American Chemical Society: Washinton, DC, 1993.

(42) Su, Y. S.; Ying, J. Y.; Green, W. H., Jr. *J. Catal.* **2003**, *218*, 321.

(43) Couwenberg, P. M.; Chen, Q.; Marin, G. B. *Ind. Eng. Chem. Res.* **1996**, *35*, 3999.

(44) DeBoy, J. M.; Hicks, R. F. *J. Chem. Soc., Chem. Commun.* **1988**, 982.

JP9001302